Available online at www.sciencedirect.com
ScienceDirect
Trans. Nonferrous Met. Soc. China 35(2025) 392−404
Transactions of Nonferrous Metals Society of China
www.tnmsc.cn

Effect of pre-aged NiTi particle layer on phase-transition behavior and damping performance of 5052Al alloy

Chao-yi DING[1,2], Hong-jie JIANG[1,2], Jia-qiang HUANG[3],
Chong-yu LIU[1], Hong-feng HUANG[1], Shu-hui LIU[2], Li-li WEI[2]

1. School of Materials Science and Engineering, Guilin University of Technology, Guilin 541004, China;
2. Key Laboratory of New Processing Technology for Nonferrous Metal & Materials, Ministry of Education, Guilin University of Technology, Guilin 541004, China;
3. School of Mechanical and Electrical Engineering, Guilin University of Electronic Technology, Guilin 541004, China

Received 15 June 2023; accepted 26 February 2024

Abstract: The insufficient damping capabilities of aluminum alloy under low temperatures (<120 °C) were addressed by developing high-damping laminated composites of NiTip/5052Al. This is achieved through the incorporation of varied pre-aging states of NiTi particles into the 5052Al matrix using a rolling composite technique. The aim is to enhance the application scope of aluminum alloy for vibration and noise reduction. The results demonstrated a distinct and integrated interface between the particle layer and the 5052Al alloy, with numerous interparticle interfaces within the particle layer. Increasing the aging temperature of the NiTi particles from 450 to 550 °C shifted the phase transition peaks of the composites to lower temperatures. The damping capacity of the laminated NiTip/5052Al composites notably surpasses that of the 5052Al alloy. At 28 and 66 °C, the phase transformation damping peaks of the pre-aged NiTi particle layer reinforced 5052Al matrix composites are 1.93 and 2 times those of the 5052Al alloy at the corresponding temperatures, respectively. The collaborative impact of interparticle interface damping mechanism and the phase transformation damping mechanism of NiTi-reinforced particles significantly amplify the low-temperature damping performance of the laminated NiTip/5052Al composites.

Key words: pre-aging; NiTi particle layer; 5052Al alloy; phase-transition behavior; damping performance

1 Introduction

With the advancements in shipbuilding technology, reducing vibration and noise has become a critical concern in the design of submarines and ships. The high-speed operation of submarines and ships often generates intense noise and vibration, which can have adverse effects on their service life, comfort, and safety [1]. Utilizing high-damping alloys in design and manufacturing processes stands out as a highly effective strategy for mitigating vibration and noise in submarines and ships [2]. The 5xxx series (Al−Mg) aluminum alloy, distinguished by its low density, high specific strength, and exceptional corrosion resistance [3,4,5], is preferred in the shipbuilding industry due to its advantageous properties [6,7]. However, the inherent damping performance of the 5xxx aluminum alloy is relatively limited, which hampers its application in vibration and noise reduction efforts [8]. Therefore, enhancing the damping performance of the 5xxx series aluminum alloy is crucial for expanding its potential applications in the shipbuilding industry.

Dislocations, grain boundaries, and interface

Corresponding author: Hong-jie JIANG, Tel: +86-773-5896672, E-mail: jhj2014@glut.edu.cn
DOI: https://doi.org/10.1016/S1003-6326(24)66687-2

damping mechanisms are key to improving the damping capacity of aluminum matrix composites. Increasing the number of movable dislocations, grain boundaries, and interfaces within the aluminum matrix significantly enhances the damping properties of the composites [9−11]. Particle-reinforced aluminum matrix composites typically manifest a heightened dislocation density than aluminum alloys, and the introduction of reinforcing particles generates multiple-phase interfaces within the aluminum matrix composites. These dislocations, coupled with interface-induced damping behaviors, contribute to the enhanced damping properties of the composites [12,13]. Furthermore, one of the key factors that contribute to the improved damping performance of aluminum matrix composites is the intrinsic damping contribution of the reinforcing phase [14]. Despite progress in enhancing the high-temperature damping performance of aluminum alloys through composite technology, achieving substantial improvement in their low-temperature damping performance remains a persistent challenge.

NiTi alloy is known for its excellent low-temperature damping property and martensite transformation characteristics, and typically exhibits phase-transition damping temperatures below 100 °C [15,16]. During the martensite transformation in NiTi alloy, the interface effects of austenite−martensite phases, movement of martensite twin boundaries, and the transformation itself contribute to phase transformation damping, resulting in distinct damping peaks [17,18]. As a result, the alloy demonstrates outstanding damping performance in the low-temperature range [19,20]. Furthermore, reports indicate that the phase transformation damping temperature range of NiTi alloy can be effectively adjusted through aging treatment [21]. For example, SONG et al [22] observed an internal friction peak corresponding to the $B2 \rightarrow R$ transformation at 35 °C after aging $Ni_{50.8}Ti_{49.2}$ alloy at 400 °C for 0.2 h. When the aging temperature was increased to 550 °C, the internal friction peak temperature decreased to 25 °C. Therefore, incorporating aged NiTi particles into the aluminum matrix as reinforcing particles is anticipated to enhance and adjust the low-temperature damping performance of the aluminum alloy by leveraging the phase transformation damping characteristics of NiTi particles, which is conducive to broadening the application range of aluminum alloy in vibration and noise reduction. However, how to use NiTi reinforced particles to improve and regulate the low-temperature damping performance of 5xxx series aluminum alloy remains to be further studied.

In this study, laminated NiTip/5052Al composites were fabricated using rolling composite technology to incorporate NiTi granular layers with different aging states into 5052Al plates. In addition, the microstructure, phase composition and phase transformation characteristics of the composites were also analyzed, and the effects of NiTi particle layers in different aging states on the mechanical properties and damping properties of the alloys were studied. This research could provide a new strategy for the design and preparation of high-damping aluminum alloys for shipbuilding applications.

2 Experimental

The materials used in this work included a commercial 5052-H32 Al plate with a thickness of 1.6 mm as the base material. Reinforcing particles of $Ni_{50.8}Ti_{49.2}$ (particle size: 10−30 μm) with a spherical morphology, and pure Al particles (particle size: 10−30 μm) with an approximately spherical morphology served as the bonding material within the granular layer. The morphologies of the $Ni_{50.8}Ti_{49.2}$ and pure Al particles are depicted in Figs. 1(a) and (b), respectively, and the nominal compositions of the pure Al particles and 5052-H32 Al plates are detailed in Table 1.

Two sets of original NiTi particles (as-NiTip) were subjected to a vacuum tube furnace under an argon atmosphere and aged for 3 h at temperatures of 450 and 550 °C, respectively. The aged samples were then air-cooled to obtain the 450-NiTip and 550-NiTip samples with different aging states. These samples were mixed with pure Al particles at a volume ratio of 2:3 for 6 h in a V-mixer, resulting in an approximate 6% volume fraction of NiTi particles in the Al matrix composites. Subsequently, the 5052Al plate was annealed at 350 °C for 1 h, followed by surface sanding using 800# sandpaper and cleaning with absolute ethanol. The prefabricated 450-NiTip and 550-NiTip mixed particles were evenly placed between two 5052Al plates, to create two groups of composite panels.

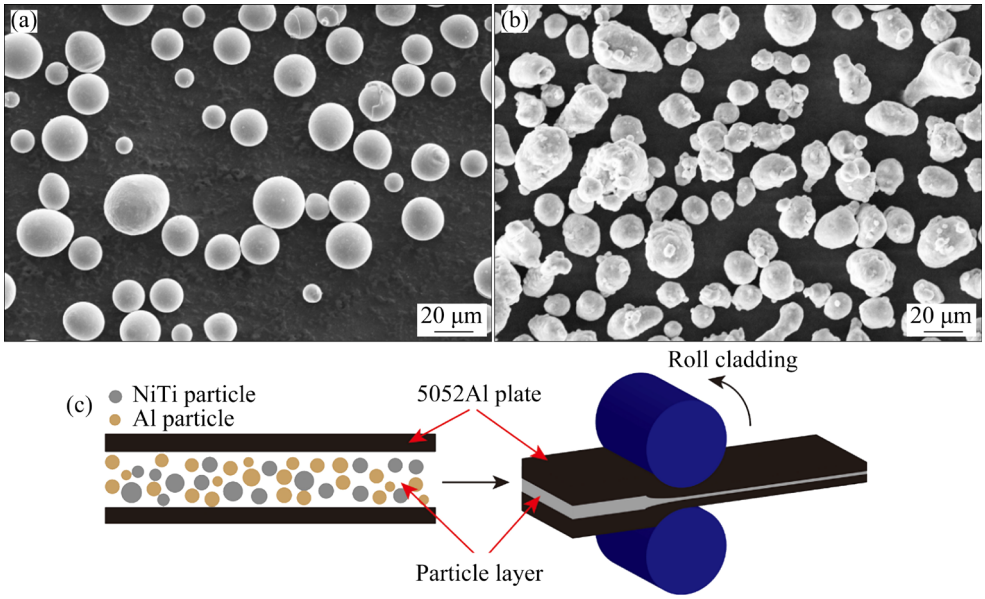

Fig. 1 SEM images of NiTi particles (a) and Al particles (b), and schematic diagram of rolling process (c)

Table 1 Chemical compositions of Al particle and 5052Al plate (wt.%)

Sample	Si	Fe	Cu	Mn	Mg	Zn	Cr	Al
Al particle	0.25	0.03	0.05	0.03	0.03	0.05	−	Bal.
5052Al plate	0.25	0.5	0.1	0.1	2.2−2.8	0.1	0.15−0.35	Bal.

These panels were then rolled at room temperature with a rolling speed of 10 mm/s and a reduction ratio of 50%−55%, forming laminated 450-NiTip/5052Al and 550-NiTip/5052Al composites, referred to as the NTAC2 and NTAC1 samples, respectively. The rolling process is depicted in Fig. 1(c).

The microstructure and elemental distribution of the laminated NiTip/5052Al composites were examined using a Hitachi S4800 scanning electron microscope (SEM) equipped with energy-dispersive spectroscopy (EDS). The phase composition analysis of the samples was conducted using an X'Pert PRO X-ray diffractometer (XRD). The phase transition behavior of the 5052Al alloy, NiTi particles, and laminated composites was analyzed using a TA DSC 25 differential scanning calorimeter (DSC) with a heating and cooling rate of 10 °C/min at temperature of −80 to 120 °C. Mechanical properties of the 5052Al alloy and laminated composites were tested at a strain rate of 2×10^{-4} s^{-1}. A Shimadsu AGS-X-20 kN universal testing machine with an extensometer was employed for the tests at room temperature. Test samples were machined from the RD−TD plane, and each group included at least three samples with a gauge length of 21 mm and a cross-section of 3 mm × 1.5 mm to ensure better reliability. The damping performance of the 5052Al alloy and laminated composites was assessed in single cantilever vibration mode using a Netzsch 242E dynamic mechanical analyzer (DMA). Test samples of 30 mm × 4 mm × 1.2 mm were used for the damping tests. For the constant temperature damping performance test, the frequency (f) was set to be 1 Hz, the amplitude (A) ranged from 0.1 to 150 μm, and the temperature (T) was maintained at 25 °C. In the variable temperature damping test (−80 to 360 °C), the frequency (f) was set to be 1 Hz for the low temperature range and 0.1−150 Hz for the high temperature range, respectively. The amplitude (A) was 10 μm, and the heating and cooling rate was 5 °C/min.

3 Results and discussion

3.1 Microstructure

Figure 2 shows the morphology of the laminated NiTip/5052Al composites. The granular layer exhibits excellent bonding with the upper and lower aluminum substrates, with no cracks observed

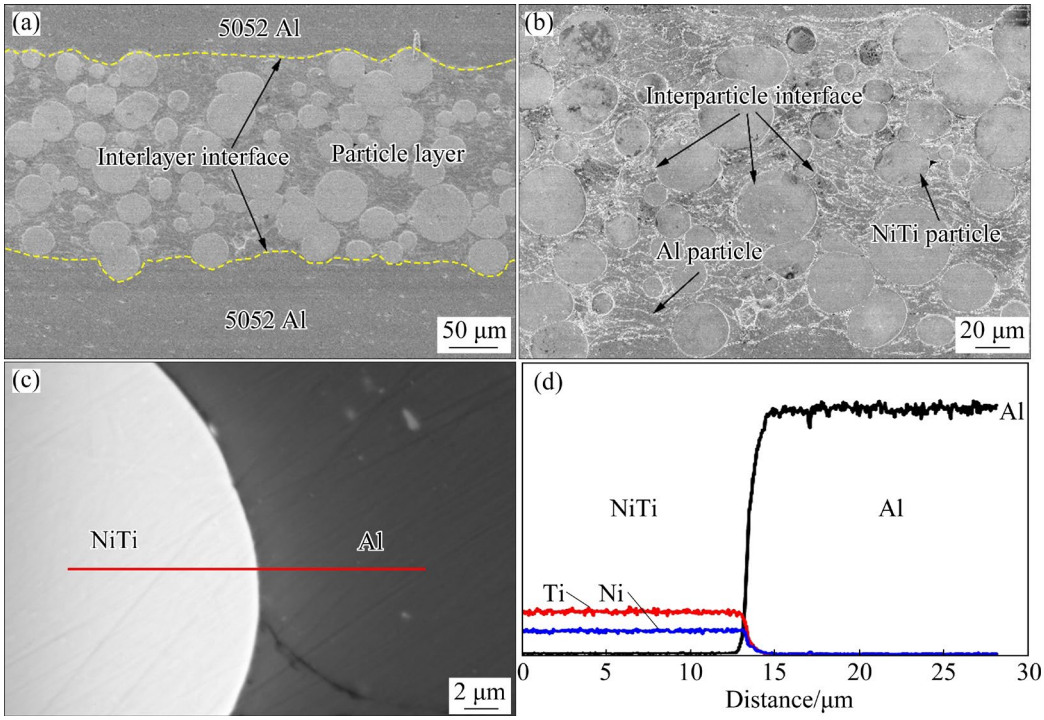

Fig. 2 SEM images of NTAC1 sample: (a) Morphology of corroded sample; (b) Local enlarged view in (a); (c) Morphology of uncorroded sample; (d) Scanning element distribution of line in (c)

at the interface between the layers. Nevertheless, small pores were observed at the interlayer interface and among the intergranular particles. The NiTi particles within the particle layer were uniformly distributed without agglomeration. In the granular layer, numerous interfaces are observed, including Al/Al intergranular interfaces, NiTi/NiTi intergranular interfaces, and NiTi/Al intergranular interfaces. Due to the high hardness and deformation resistance of the NiTi particles, their original spherical shape is maintained during the rolling process. In contrast, the Al particles, with lower hardness and deformation resistance, experience extrusion and deformation, resulting in elongated shapes, as observed in Figs. 2(a) and (b). The interface of each element is clearly defined, with no noticeable diffusion layer or observable interfacial reaction products, as shown in Figs. 2(c) and (d). This result suggests that there is no elemental diffusion or interfacial reactions at the interlayer interface between the granular layer and the 5052Al matrix, as well as at the NiTi/Al interparticle interface within the granular layer during the cold rolling process. The primary bonding mechanism of the laminated composites is attributed to mechanical bonding.

Figure 3 shows the XRD patterns of the 5052Al alloy, NiTi particles, and laminated NiTip/5052Al composites. In the 5052Al alloy, only diffraction peaks corresponding to the α-Al phase are observed. The diffraction pattern of the as-NiTip and 550-NiTip samples exclusively reveals the $B2$ phase of the NiTi alloy. The diffraction pattern of the 450-NiTip sample includes both the NiTi (R) phase and the NiTi ($B2$) phase. This observation is consistent with the subsequent DSC test results, indicating that the 450-NiTip sample undergoes the

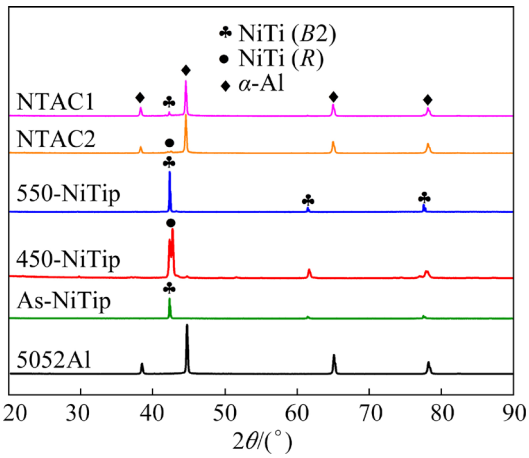

Fig. 3 XRD patterns of 5052Al alloy, NiTi particles and laminated composites

R-phase transition at room temperature; hence the prominent diffraction peak indicates the *R*-phase bimodal structure. However, the as-NiTip and 550-NiTip samples do not undergo a phase transition during cooling to room temperature, resulting in them being entirely composed of the NiTi (*B*2) phase (Fig. 4(a)). Following the rolling composite process, the NTAC2 sample comprised the *α*-Al phase and the NiTi (*R*) phase, while the NTAC1 sample consisted of *α*-Al phase and NiTi (*B*2) phase. indicating that no new phases formed during the rolling process.

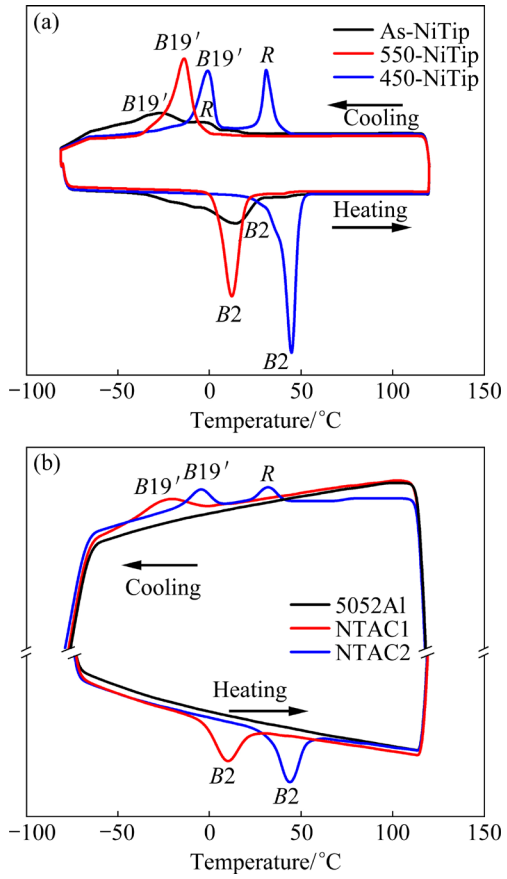

Fig. 4 DSC curves of samples: (a) NiTi particles with different aging states; (b) Laminated composites and 5052Al alloys

3.2 Phase transition characteristics

In Fig. 4(a), the DSC curves illustrate the behavior of NiTi particles in various aging states. Comparative analysis with the as-NiTip samples revealed that aging treatment of the 550-NiTip and 450-NiTip samples led to a narrow phase-transition temperature range and a notable increase in the intensity of the phase transition peak. During the heating process, all three samples (as-NiTip, 550-NiTip and 450-NiTip) exhibited a phase transition peak corresponding to the *B*19'→*B*2 phase transition of the NiTi alloy. During the cooling process, both the as-NiTip and 450-NiTip samples exhibited two-phase transition peaks for the *R* and *B*19'. In the 550-NiTip sample, only one *B*19' phase transition peak was observed at a temperature of −15 °C, corresponding to the *B*2→*B*19' transition process, with no *R* phase transition peak observed. During the aging process of the NiTi particles at 550 °C, the Ni_4Ti_3 phase in the NiTi matrix gradually transforms into Ni_3Ti_2 and Ni_3Ti phases. Concurrently, the Ni_4Ti_3 precipitates undergo dissolution at this temperature, leading to the absence of the *R* phase transition [20,23,24]. The partial dissolution of Ni-rich precipitates in the 550-NiTip sample increases the Ni content in the NiTi matrix, causing the phase transition peak temperature to shift toward lower temperatures [24], resulting in a lower phase transition peak temperature than that of the 450-NiTip sample.

Figure 4(b) displays the DSC curves of the laminated NiTip/5052Al composites and the 5052Al alloy. Within the temperature range of −80 to 120 °C, the 5052Al alloy does not undergo any phase transformation. In contrast, the laminated composites exhibit distinct phase transformation characteristics of the NiTi particles. The NTAC1 and NTAC2 samples underwent a one-step *B*19'→*B*2 phase transition during the heating process. During the cooling process, the NTAC1 sample undergoes a one-step *B*2→*B*19' phase transition, and the NTAC2 sample demonstrates a two-step phase transition of *B*2→*R* and *R*→*B*19'. It is evident that the laminated composites follow the same phase transition sequence as their NiTi-reinforced particles. The composites consisted of both NiTi-reinforced particles and a 5052Al matrix that lacked phase transition characteristics, resulting in significantly weak phase transition peak strength in the composite compared to the NiTi-reinforced particles.

3.3 Mechanical properties

Figure 5 shows the engineering stress−strain curves of the laminated NiTip/5052Al composites and the 5052Al alloy. The NTAC1 sample demonstrated a yield strength of 252 MPa, a tensile strength of 277 MPa, and an elongation of 5.72%. Similarly, the NTAC2 sample exhibited a yield strength of 264 MPa, a tensile strength of 278 MPa,

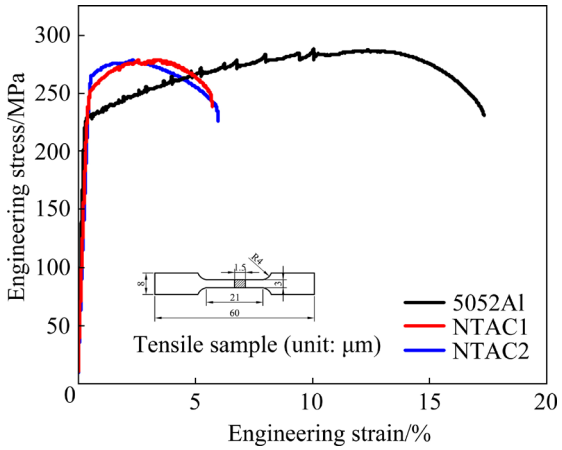

Fig. 5 Engineering stress−strain curves of laminated composites and 5052Al alloy

and an elongation of 5.98%. The different aging states of the NiTi particles have a slight impact on the mechanical properties of the composites. In comparison, the 5052Al alloy exhibited a yield strength of 229 MPa, a tensile strength of 286 MPa, and an elongation of 17.32%. Compared with that of the 5052Al alloy, the yield strength of the laminated NiTip/5052Al composite is greater, and the tensile strength is close to that of the alloy. However, there was a substantial decrease in the elongation of the composite compared with the 5052Al alloy.

Figure 6 shows the fracture morphology of the NTAC1 sample. As depicted in Figs. 6(a) and (b), the overall appearance of the composite fracture is concave, with observable cracking occurring between the intermediate granular layer and the aluminum matrix on both sides. This behavior is attributed to stress concentration at the contact layer between the NiTi granular layer and the 5052 aluminum matrix during the tensile process. The plastic deformation capacity of the granular layer is not as robust as that of the aluminum matrix, leading to interlayer cracks due to strain mismatch. With the transfer of load, these interlayer cracks continue to propagate until the particle layer fractures. The propagation of interfacial cracks requires additional energy, resulting in increased overall energy absorption of the composites. This contributed to the increase in the yield strength of the laminated composites, surpassing that of the 5052Al alloy [25].

In Fig. 6(c), pits are observed within the granular layer, and the NiTi particles within the particle layer maintain their complete spherical morphology. This indicates that the NiTi particles do not deform during the process of interlayer cracking and particle layer fracture but rather disengage from adjacent Al particles or NiTi particles. Additionally, cleavage fracture is observed

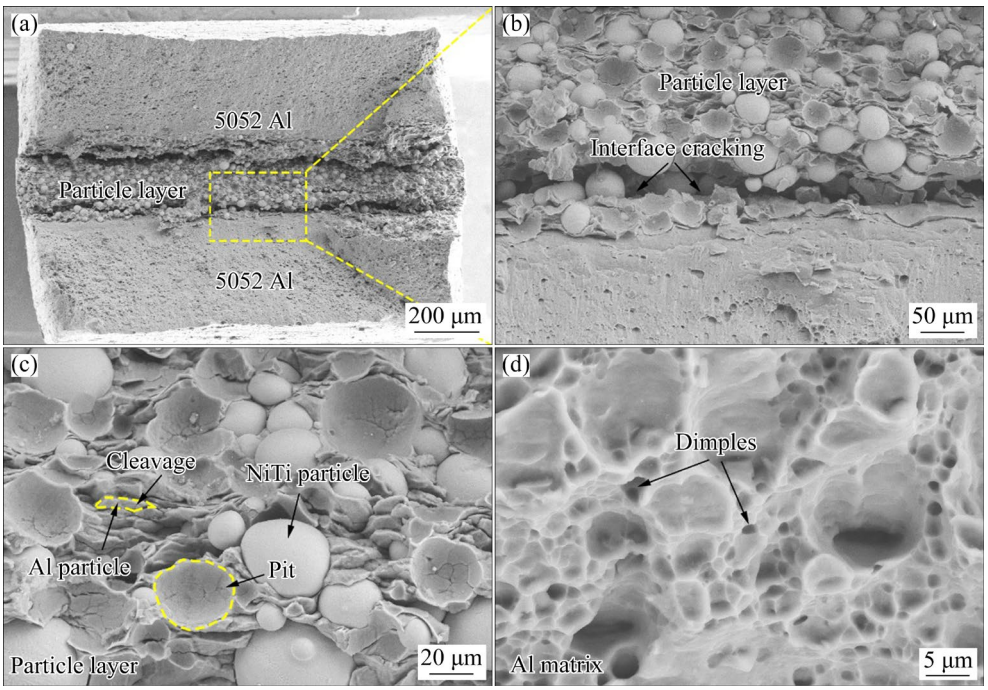

Fig. 6 Fracture morphology of NTAC1 sample: (a) Overall morphology; (b) Local amplification of (a); (c) Granular layer; (d) Aluminum matrix

between the Al particles within the particle layer. This suggests that the binding force between Al particles is stronger than that between adjacent NiTi particles or NiTi/Al particles. Therefore, the fracture mechanism of the particle layer is primarily brittle, resulting in a noticeable reduction in the elongation of the composites compared to the 5052Al alloy. On the fracture surface of the aluminum matrix of the composites, numerous small dimples are observed, indicating a ductile fracture mode of the aluminum matrix (Fig. 6(d)).

3.4 Damping behavior

Figure 7 shows the internal friction−strain curves of the laminated NiTip/5052Al composites and the 5052Al alloy. With increasing strain, the internal frictions of all three materials increase. When the strain is below 0.05%, there is a slight difference in the internal friction between the composites and the Al matrix. However, as the strain continues to increase, the internal friction of the composites gradually surpasses that of the 5052Al alloy. For interfaces in a weak binding state, the energy loss (η) due to friction during the cyclic loading of the reinforcing phase with the matrix interface can be analyzed as follows [26]:

$$\eta = \frac{3\pi}{2}\mu k\gamma\varphi \tag{1}$$

where μ represents the friction coefficient between NiTi particles and Al, k denotes the stress concentration factor at the interface between the reinforcement phase and the metal matrix, γ is the correction factor, and φ is the volume fraction of added NiTi particles. During cyclic loading, the strain mismatch between NiTi particles and the Al matrix leads to stress concentration at the particle interface. Moreover, the bimetallic interface in a mechanically bonded state typically exhibits a high friction coefficient. Consequently, the damping performance improvement in the composites is primarily attributed to the interface damping caused by NiTi−Al interface slip. When the strain reaches 0.2%, the internal friction of the NTAC1 sample reaches 0.0258, which is increased by 90% compared to that of the Al matrix (0.0136).

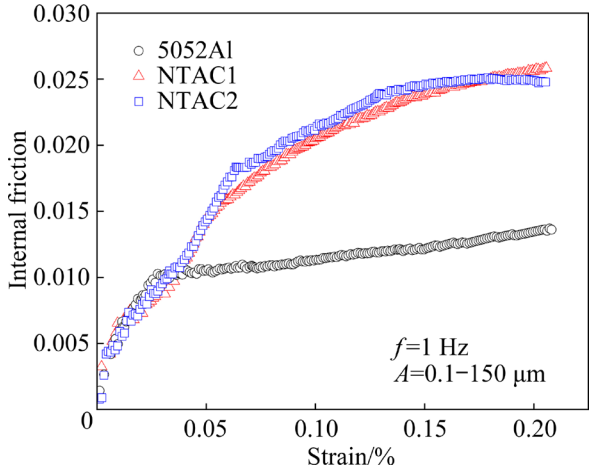

Fig. 7 Internal friction−strain curves of laminated composites and 5052Al alloy

Figure 8(a) shows the internal friction−temperature curves of laminated the NiTip/5052Al composites and 5052Al alloy within the temperature range of 120−350 °C. From the graph, it is evident that as the temperature increases, the internal friction gradually rises for both the 5052Al alloy and the laminated NiTip/5052Al composites. This can be attributed to the contribution of the grain boundary damping behavior of the aluminum matrix, which improves the damping properties of the 5052Al alloy and the aluminum matrix composites. However, when the temperature is higher than 320 °C, the damping properties of 5052Al alloy and laminated NiTip/5052Al composite decrease significantly. Under high-temperature conditions (120−350 °C), the laminated NiTip/5052Al composites exhibit superior damping performance compared to the 5052Al alloy. The granular layer of the laminated NiTip/5052Al composites contains numerous interfaces, including NiTi/Al, Al/Al, and NiTi/NiTi particle interfaces. During high-temperature deformation, these interfaces experience micro-slip, inducing interface damping behavior. This effect contributes to the enhancement of the high-temperature damping performance of the laminated composites.

Figure 8(b) shows the internal friction−temperature curves of NTAC2 samples at various testing frequencies ranging from 120 to 360 °C. It is evident that as the frequency increases, the internal friction of the composites steadily decreases. When the frequency decreases under the same temperature and amplitude conditions, the number of mobile dislocations in alloys increases with decreasing frequency at a constant temperature and amplitude, because more pinned dislocations could be activated at the low frequency stress [27]. As a result, the laminated composites exhibit the best

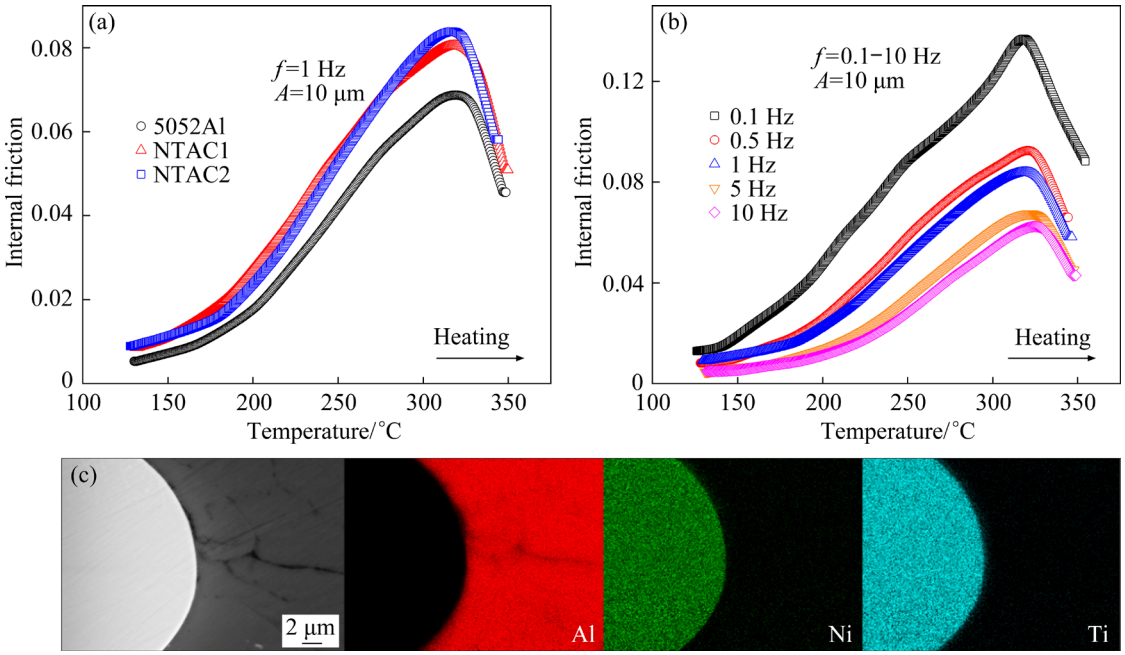

Fig. 8 Internal friction−temperature curves of laminated composites and 5052Al alloy at 120−360 °C (a), internal friction−temperature curves of NTAC2 samples at different test frequencies (b), and SEM image of NTAC2 sample after high-temperature damping test and area scanning element distribution maps (c)

damping performance at a testing frequency of 0.5 Hz. Furthermore, all the NTAC2 samples tested at different frequencies exhibit damping peaks at approximately 320 °C.

Figure 8(c) shows the SEM image and area scanning element distribution of the NTAC2 sample after a high-temperature damping test. The results reveal very slight elemental diffusion between the NiTi particles and the Al matrix. However, there is no sign of an interfacial reaction layer, indicating virtually no reaction between NiTi particles and the 5052Al alloy. At high-temperatures (>320 °C), the damping performance of the composites and 5052Al matrix decreases rapidly. The likely reason is that the internal grains of the material undergo recrystallization and growth at high temperatures, reducing the contribution of grain boundary damping, and resulting in a decline in the damping performance of the material [15,28].

Figure 9 shows the internal friction−temperature curves for the laminated NiTip/5052Al composite and the 5052Al alloy over the temperature range of −80 to 120 °C. The diagram reveals distinct internal friction peaks in the laminated composites during both the heating and cooling processes. These internal friction peaks are caused by the phase transition behavior of NiTi reinforced particles in the composites [18,29]. The low-temperature damping performance of the laminated NiTip/5052Al composites is significantly superior to that of the 5052Al alloy. During vibration deformation, the weakly bonded interfaces between particles in the composite experience micro-slip motion due to strain mismatch and low mechanical binding force, resulting in interface damping behavior. This improves the damping performance of the composite. The coupling effect between interfacial damping among particles and the phase transformation damping mechanism of NiTi-reinforced particles contributed to the excellent low-temperature damping properties of the laminated NiTip/5052Al composites.

During the heating process, the NTAC1 sample exhibited an internal friction peak at 28 °C, with an internal friction of 0.0083, which was 1.93 times that of the 5052Al alloy at the corresponding temperature (0.0043). The NTAC2 sample exhibited an internal friction peak at 66 °C, with an internal friction of 0.0096, which is twice that of the corresponding temperature of the 5052Al alloy (0.0048). These peaks correspond to the $B19' \rightarrow B2$ phase transition process in the 450-NiTip and 550-NiTip samples, respectively. During the cooling

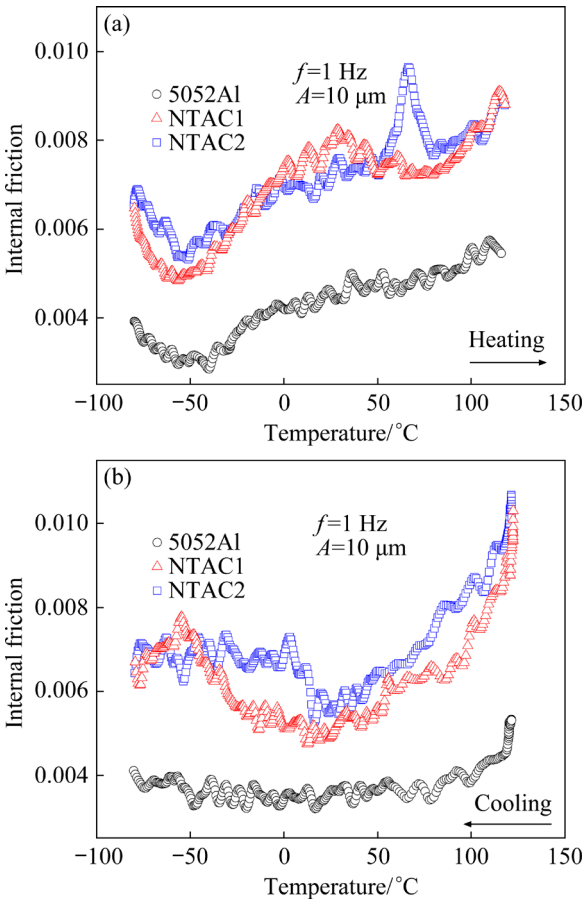

Fig. 9 Internal friction−temperature curves of laminated composites and 5052Al alloy within range of −80 to 120 °C: (a) Heating process; (b) Cooling process

process, the NTAC1 sample exhibits a phase transition internal friction peak temperature of −54 °C, with an internal friction of 0.0079, corresponding to the *B*2→*B*19' phase transition process in the 550-NiTip sample. During the cooling process, the NTAC2 sample demonstrates the presence of *R* phase high damping platform resulting from the occurrence of *R* phase transition in the NiTi-reinforced particles [30]. These findings indicate that the aging treatment of NiTi particles at different temperatures effectively controlled the phase transformation damping temperature range of the laminated NiTip/5052Al composites, enhancing the higher damping properties within the low-temperature range of −80 to 120 °C.

The rule of mixtures (ROM) was used to assess the impact of specific components in composite materials [31]. The damping performance of the laminated NiTip/5052Al composites can be evaluated by [32]

$$\eta_c=\eta_p V_p+\eta_m V_m+\eta_i V_i \quad (2)$$

where η_c represents the damping performance of the composite material, η_p, η_m and η_i represent the damping of NiTi particles, 5052Al matrix and interface, respectively, and V represents their respective volume fractions. It can be inferred that the inclusion of NiTi particles enhances the damping performance of the composites. As the volume fraction of the NiTi particles in the aluminum matrix composite increases, such as the particle layer thickness, the composites are expected to achieve better overall damping performance. This improvement is attributed to the high intrinsic damping performance of NiTi alloy and the weak bonding interface damping behavior between NiTi and Al particles. Based on the ROM, increasing the thickness of the aluminum plate also enhances the damping properties of the composites, but this enhancement may be limited due to the poor low-temperature damping properties of aluminum alloys.

Figure 10 shows the storage modulus−temperature curves for the laminated NiTip/5052Al composites and the 5052Al alloy. As the temperature increases, the storage modulus of both the 5052Al alloy and the laminated NiTip/5052Al composites gradually decreases. The storage modulus of the NTAC1 and NTAC2 samples exhibits minimal difference, indicating that the aging state of the NiTi particles slightly influences the storage modulus of the laminated NiTip/5052Al composites. Moreover, the laminated composites also exhibit a higher storage modulus than the 5052Al alloy. Previous reports suggest that an increase in residual stress within the alloy contributes to an enhancement in its storage modulus [28]. During the rolling composite process, interparticle compression takes place within the granular layer of the laminated NiTip/5052Al composites, which leads to an increase in the dislocation density within the particle layer and at the interlayer interface. Consequently, this results in the generation of residual stress within the composites, thereby enhancing the storage modulus.

Figure 11 shows the E_{IF}−temperature curves for the laminated NiTip/5052Al composites and the 5052Al alloy, where E_{IF} is defined as the product of the storage modulus and the internal friction (IF, f_i), which serves as a measure of the comprehensive

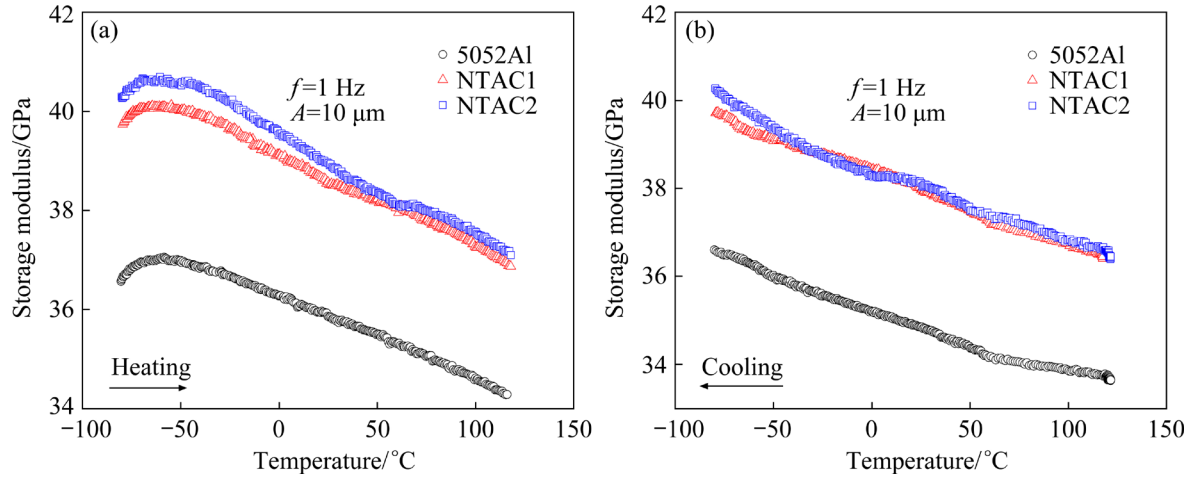

Fig. 10 Storage modulus−temperature curves of laminated composites and 5052Al alloy in range of −80 to 120 °C: (a) Heating process; (b) Cooling process

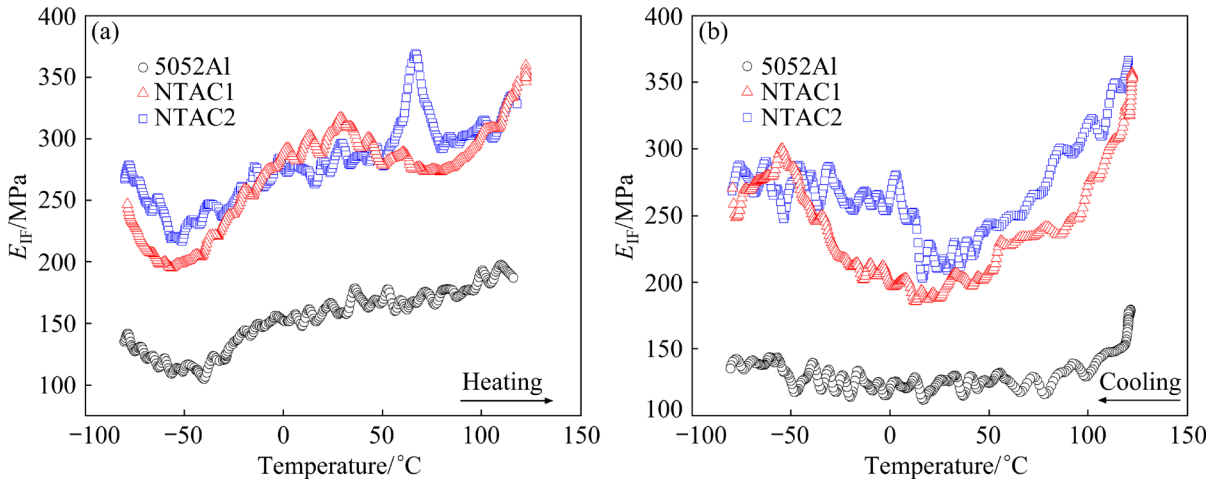

Fig. 11 E_{IF}−temperature curves of laminated composites and 5052 Al alloy: (a) Heating process; (b) Cooling process

damping performance [33]. The calculation formula for E_{IF} is

$$E_{IF}=E_S f_i \quad (3)$$

In Eq. (3), the storage modulus of the material is denoted as E_S. The graph illustrates that the laminated composites show a considerably higher E_{IF} value compared with the 5052Al alloy, indicating their superior overall damping capacity. At a temperature of 66 °C, the NTAC2 sample shows E_{IF} value of 369 MPa, which is 2.22 times that of the 5052Al alloy (166 MPa). Similarly, at a temperature of 29 °C, the E_{IF} of the NTAC1 sample was measured as 318 MPa, which is 2.02 times that of the 5052Al alloy (157 MPa). These data imply that the potential of laminated composites holds promise as lightweight damping materials in various engineering applications.

4 Conclusions

(1) Laminated NiTip/5052Al composites that exhibit high damping properties at low temperatures, are successfully produced through rolling composite technology. Numerous mechanically bonded inter-particle interfaces are distributed in the particle layer of the composites, characterized by distinct boundaries and no evidence of element diffusions.

(2) Laminated NiTip/5052Al composites exhibit NiTi phase transition characteristics, which are absent in aluminum alloys. With an increase in the aging temperature of the NiTi particles, the phase transition peak shifts towards low

temperatures, facilitating tuning of the phase-transition damping temperature range in the composites. The yield strength of laminated NiTip/5052Al composites is higher than that of 5052Al alloy, and the fracture morphology of the composite exhibits a combination of ductile and brittle fracture characteristics.

(3) Compared with those of the 5052Al alloy, the enhanced low-temperature damping performance and overall damping efficiency of the laminated NiTip/5052Al composites are attributed to the synergistic effect of phase transition damping due to the NiTi particles in the particle layer and interface damping from interparticle slip. Consequently, these composites are expected to be advantageous in the shipbuilding sector as high-damping and lightweight structural materials.

CRediT authorship contribution statement

Chao-yi DING: Investigation, Characterization, Data curation, Writing – Review & editing, Funding acquisition; **Hong-jie JIANG:** Conceptualization, Characterization, Formal analysis, Data curation, Writing – Review & editing, Supervision, Funding acquisition; **Jia-qiang HUANG:** Investigation, Characterization, Writing – Review; **Chong-yu LIU:** Writing – Review & editing; **Hong-feng HUANG:** Investigation and review; **Shu-hui LIU:** Investigation and characterization; **Li-li WEI:** Editing and supervision.

Declaration of competing interest

The authors declare that they have no known competing financial interests or personal relationships that could have appeared to influence the work reported in this paper.

Acknowledgments

This work was supported by the National Natural Science Foundation of China (No. 52061011), the Guangxi Natural Science Foundation, China (No. 2022GXNSFAA035574), and Innovation Project of Guangxi Graduate Education, China (No. YCSW2023361).

References

[1] LARA P A, BRUCK H A. Experimental investigation of high frequency pulse loading on fatigue crack growth in 5052−H32 series aluminum [J]. International Journal of Fatigue, 2021, 153: 106476.

[2] HUANG Guo-qiang, SHEN Yi-fu. The effects of processing environments on the microstructure and mechanical properties of the Ti/5083Al composites produced by friction stir processing [J]. Journal of Manufacturing Processes, 2017, 30: 361−373.

[3] ZHANG Lei, LIU Chong-yu, ZHANG Bing, HUANG Hong-feng, XIE Hai-yan, CAO Kai. Mechanical properties of Al−Mg alloys with equiaxed grain structure produced by friction stir processing [J]. Materials Chemistry and Physics, 2023, 294: 127010.

[4] SON K, KASSNER M E, LEE T K, LEE J W. Mg effect on the cryogenic temperature toughness of Al−Mg alloys [J]. Materials & Design, 2022, 224: 111336.

[5] LI Meng-jia, ZHANG En-gui, LIU Shu-yu, WANG Xiang-dong, SHI Yun-jia, WU Jian-zheng, GUAN Shao-kang. Microstructure and properties of Al−2Mg−0.5Mn alloy with narrow crystallization temperature range realized by adding trace elements [J]. Transactions of Nonferrous Metals Society of China, 2023, 33(10): 2898−2912.

[6] GUO Cheng, CHEN Yi-fei, ZHANG Hai-tao, JI Hai-peng, WU Zi-bin, LIU Xin-gang, NAGAUMI H. Synchronous improvement of mechanical properties and corrosion resistance of novel heat-treatable 5xxx aluminum alloy by non−isothermal ageing [J]. Journal of Alloys and Compounds, 2023, 939: 168770.

[7] DENG Ying, ZHU Xin-wen, LAI Yi, GUO Yi-fan, FU Le, XU Guo-fu, HUANG Ji-wu. Effects of Zr/(Sc+Zr) microalloying on dynamic recrystallization, dislocation density and hot workability of Al−Mg alloys during hot compression deformation [J]. Transactions of Nonferrous Metals Society of China, 2023, 33(3): 668−682.

[8] LI Zhen-zhen, YAN Hong-ge, CHEN Ji-hua, XIA Wei-jun, ZHU Hua-ming, SU Bin, LI Xin-yu, SONG Min. Enhancing damping capacity and mechanical properties of Al−Mg alloy by high strain rate hot rolling and subsequent cold rolling [J]. Journal of Alloys and Compounds, 2022, 908: 164677.

[9] JIANG Hong-Jie, ZHANG Bing, LIU Chong-Yu, YANG Zhen-Xing, MA Zong-Yi. Mechanical and damping behavior of age-hardened and non-age-hardened Al alloys after friction stir processing [J]. Acta Metallurgica Sinica (English Letters), 2019, 32(9): 1135−1141.

[10] ZHANG Zhi-hao, XIAO Fei, WANG You-wei, JIANG Yan-bin. Mechanism of improving strength and damping properties of powder-extruded Al/Zn composite after diffusion annealing [J]. Transactions of Nonferrous Metals Society of China, 2018, 28(10): 1928−1937.

[11] JOSHUA T O, ALANEME K K, BODUNRIN M O, OMOTOYINBO J A. On the microstructure, mechanical behaviour and damping characteristics of Al−Zn based composites reinforced with martensitic stainless steel (410L) and silicon carbide particulates [J]. International Journal of Lightweight Materials and Manufacture, 2022, 5(3): 279−288.

[12] LV Zhao-zhao, LIU Xiao-bo, WANG Jing-feng, DONG Sheng-quan, GUO Yong-chun, SHA Jian-jun, LIN Guan-zhang. Enhancing damping capacity and mechanical properties of aluminum matrix composites by the synergistic strengthening of SiC particles and carbon fibers [J].

Materials Letters, 2023, 334: 133728.

[13] YANG Gan-ting, HAN Yi-fan, LU An-liang, GUO Qiang. Enhanced damping capacity of nanolaminated graphene (reduced graphene oxide)/Al−Mg−Si composite [J]. Composites Part A: Applied Science and Manufacturing, 2022, 156: 106887.

[14] VENKATESWARA R K, BHEEKYA N R, RAO G R, MADHUSUDHAN R G, AROCKIA K R. Microstructure and damping capacity of AA6061/graphite surface composites produced through friction stir processing [J]. Composites Communications, 2020, 20: 100352.

[15] YU Ben-quan, YUAN Wen-hui, XU Qiang, GU Yun-fang-zi, XIAO Ming-ming, XU Guo-fu, LI Zhou, XIAO Zhu, XIAO Zi-an. Comparison of nickle release and cytocompatibility between porous and dense NiTi alloy [J]. Transactions of Nonferrous Metals Society of China, 2021, 31(12): 3814−3820.

[16] JIANG Hong-jie, KE Chang-bo, CAO Shan-shan, MA Xiao, ZHANG Xin-ping. Phase transformation and damping behavior of lightweight porous TiNiCu alloys fabricated by powder metallurgy process [J]. Transactions of Nonferrous Metals Society of China, 2013, 23(7): 2029−2036.

[17] COLUZZI B, BISCARINI A, CAMPANELLA R, MAZZOLAI G, TROTTA L, MAZZOLAI F M. Effect of thermal cycling through the martensitic transition on the internal friction and Young's modulus of a $Ni_{50.8}Ti_{49.2}$ alloy [J]. Journal of Alloys and Compounds, 2000, 310(1/2): 300−305.

[18] ZHAO Mi, SHAO Yu-man, ZHENG Wei-jie, LUO Yong-hua, QIAO Ji-chao, WU Shu-sen, YAN You-wei, GUO Wei. Tailoring the damping and mechanical properties of porous NiTi by a phase leaching process [J]. Journal of Alloys and Compounds, 2021, 855: 157471.

[19] KHALIL ALLAFI J, REN X, EGGELER G. The mechanism of multistage martensitic transformations in aged Ni-rich NiTi shape memory alloys [J]. Acta Materialia, 2002, 50(4): 793−803.

[20] ZHENG Yu-feng, JIANG Fei, LI Li, YANG Hong, LIU Yi-nong. Effect of ageing treatment on the transformation behaviour of Ti−50.9at.%Ni alloy [J]. Acta Materialia, 2008, 56(4): 736−745.

[21] HUO Xin-yu, CHEN Peng, LAHKAR S, JIN Ming-jiang, HAN Xiao-cang, SONG Yuan-wei, WANG Xiao-dong. Occurrence of the *R*−phase with increased stability induced by low temperature precipitate-free aging in a $Ni_{50.9}Ti_{49.1}$ alloy [J]. Acta Materialia, 2022, 227: 117688.

[22] SONG Yuan-wei, JIN Ming-jiang, HAN Xiao-cang, WANG Xiao-dong, CHEN Peng, JIN Xue-jun. Microstructural origin of ultrahigh damping capacity in $Ni_{50.8}Ti_{49.2}$ alloy containing nanodomains induced by insufficient annealing and low−temperature aging [J]. Acta Materialia, 2021, 205: 116541.

[23] QIN Qiu-hui, PENG Hua-bei, FAN Qi-chao, ZHANG Lan-hui, WEN Yu-hua. Effect of second phase precipitation on martensitic transformation and hardness in highly Ni-rich NiTi alloys [J]. Journal of Alloys and Compounds, 2018, 739: 873−881.

[24] KAYA I, KARACA H E, NAGASAKO M, KAINUMA R. Effects of aging temperature and aging time on the mechanism of martensitic transformation in nickel−rich NiTi shape memory alloys [J]. Materials Characterization, 2020, 159: 110034.

[25] ZHANG Xiao-bo, YU Yang-bo, LIU Bin, REN Jun-qiang. Mechanical properties and tensile fracture mechanism investigation of Al/Cu/Ti/Cu/Al laminated composites fabricated by rolling [J]. Journal of Alloys and Compounds, 2019, 805: 338−345.

[26] SRIKANTH N, GUPTA M. Estimation of elasto-thermodynamic damping in the Al/SiC system using a finite element approach [J]. Acta Materialia, 2006, 54(17): 4553−4563.

[27] JIANG Hong-jie, LIU Chong-yu, MA Zong-yi, ZHANG Xin-yu, YU Liang, MA Ming-zhen, LIU Ri-ping. Fabrication of Al–35Zn alloys with excellent damping capacity and mechanical properties [J]. Journal of Alloys and Compounds, 2017, 722: 138−144.

[28] ZHOU Gao-feng, JIANG Hong-jie, LIU Chong-yu, HUANG Hong-feng, WEI Li-li, MENG Zheng-bing. Effect of porous particle layer on damping capacity and storage modulus of AlSi30p/5052Al composites [J]. Materials Letters, 2021, 300: 130162.

[29] WU S K, LIN H C. Damping characteristics of TiNi binary and ternary shape memory alloys [J]. Journal of Alloys and Compounds, 2003, 355(1/2): 72−78.

[30] JIN Ming-jiang, SONG Yuan-wei, WANG Xiao-dong, CHEN Peng, PANG Guo-bo, JIN Xue-jun. Ultrahigh damping capacity achieved by modulating *R* phase in $Ti_{49.2}Ni_{50.8}$ shape memory alloy wires [J]. Scripta Materialia, 2020, 183: 102−106.

[31] SHI Hai-long, XU Chao, HU Xiao-shi, GAN Wei-min, WU Kun, WANG Xiao-jun. Improving the Young's modulus of Mg via alloying and compositing—A short review [J]. Journal of Magnesium and Alloys, 2022, 10(8): 2009−2024.

[32] ZHANG Jin-min, PEREZ R J, WONG C R, LAVERNIA E J. Effects of secondary phases on the damping behaviour of metals, alloys and metal matrix composites [J]. Materials Science and Engineering: R, 1994, 13(8): 325−389.

[33] LI Da-sheng, ZHANG Xin-ping, XIONG Zhi-peng, MAI Yiu-wing. Lightweight NiTi shape memory alloy based composites with high damping capacity and high strength [J]. Journal of Alloys and Compounds, 2010, 490(1/2): L15−L19.

预时效 NiTi 颗粒层对 5052Al 合金相变行为和阻尼性能的影响

丁超逸[1,2]，江鸿杰[1,2]，黄家强[3]，刘崇宇[1]，黄宏锋[1]，刘淑辉[2]，韦莉莉[2]

1. 桂林理工大学 材料科学与工程学院，桂林 541004；
2. 桂林理工大学 广西有色金属及特色材料加工教育部重点实验室，桂林 541004；
3. 桂林电子科技大学 机电工程学院，桂林 541004

摘　要：针对铝合金在低温(<120 ℃)下阻尼性能不足的问题，采用轧制复合技术，在 5052Al 基体中引入不同预时效状态的 NiTi 颗粒，制备低温高阻尼 NiTip/5052Al 层状复合材料，进一步扩大铝合金在减振降噪领域的应用。结果表明，颗粒层与 5052Al 合金之间存在清晰且结合良好的界面，颗粒层中存在大量的颗粒间界面。将掺入 NiTi 颗粒的时效温度从 450 ℃提高到 550 ℃，复合材料的相变峰向更低的温度移动。NiTip/5052Al 复合材料的阻尼性能明显优于 5052Al 合金。预时效 NiTi 颗粒层增强 5052Al 基复合材料在 28 ℃和 66 ℃时的相变阻尼峰值分别是 5052Al 合金在相应温度时的 1.93 倍和 2 倍。在振动变形过程中，NiTi 增强颗粒的相变阻尼机制和颗粒间界面阻尼机制的耦合作用显著增强了 NiTip/5052Al 复合材料的低温阻尼性能。

关键词：预时效；NiTi 颗粒层；5052 铝合金；相变行为；阻尼性能

(Edited by Xiang-qun LI)